

## Supporting Information

### Enhancement of the Characteristics and HER Activity of Molybdenum Carbide Nanosheets for the Hydrogen Evolution Reaction

Muhammad Faisal Iqbal<sup>a</sup>, Muhammad Idrees<sup>bc</sup>, Muhammad Imran<sup>d</sup>, Aamir Razaq<sup>e</sup>, Guanming  
Zhu<sup>g</sup>, Jing Zhang<sup>a\*</sup>, Zahir Muhammad<sup>f\*</sup>, Meng Zhang<sup>g\*</sup>

<sup>a</sup> College of Chemistry and Materials Science, Zhejiang Normal University, Jinhua, 321004 China

<sup>b</sup> School of Materials Science and Engineering, Dongguan University of Technology, Dongguan  
523808, PR China

<sup>c</sup> State Key Laboratory of Fire Science, University of Science and Technology of China, 96 Jinzhai  
Road, Hefei, Anhui 230026, PR China

<sup>d</sup> Department of Chemistry, Faculty of Science, King Khalid University, P.O. Box 9004, Abha,  
61413, Saudi Arabia

<sup>e</sup> Department of Physics, COMSATS University Islamabad, Lahore Campus, Lahore 54000,  
Pakistan

<sup>f</sup> Hefei Innovation Research Institute, School of Microelectronics, Beihang University, Hefei  
230013, PR China

<sup>g</sup> State Key Laboratory of Radio Frequency Heterogeneous Integration and College of Electronics  
and Information Engineering, Shenzhen University, Shenzhen 518060, China

Corresponding Authors: Meng Zhang ([zhangmeng@connect.ust.hk](mailto:zhangmeng@connect.ust.hk)), Zahir Muhammad  
([zahir@mail.ustc.edu.cn](mailto:zahir@mail.ustc.edu.cn)), Jing Zhang ([jingzhang@zjnu.edu.cn](mailto:jingzhang@zjnu.edu.cn))

## 1. Structural analysis

The survey spectrum of the Mo<sub>2</sub>C-600 showed peaks at 35.0, 247.40, 285.50, 280.60, 401.12, 532.58 and 970.80 eV (Figure S1a). Peaks appeared at 247.40, 285.50, 401.12 and 532.58 eV corresponding to the Mo-3d, C-1s, Mo-3p, N-1s and O-1s, respectively, but some shifting in peaks have been found, which may be due to no reaction and some intermediate states at the annealing temperature of 600 °C.<sup>1, 2</sup> Elemental spectrums have been illustrated in detail to evaluate the change and composition of the structure. The molybdenum elemental spectrum of the Mo<sub>2</sub>C-600 showed the binding energies peaks at 235.34 eV, which corresponds to the Mo<sup>+4</sup>-3d<sub>3/2</sub> (Figure S1b). There is only peaks on molybdenum, which is most probable from the raw precursors and incomplete reaction. The carbon elemental spectrum of the Mo<sub>2</sub>C-600 showed the binding energies peaks at 284.64, 285.60 and 287.12 eV (Figure S1c). There is a little difference between the first two peaks at 283.69 and 284.69 eV, which is revealed to the C-1s. The peaks at 286.34 eV showed that the surface of the Mo<sub>2</sub>C-600 was exposed to the environmental surface.<sup>2</sup> The survey spectrum of the Mo<sub>2</sub>C-900 showed peaks at 39.61, 230.89, 280.61, 401.12, 412.10, 532.58 and 970.79 eV (Figure S1d). Peaks appeared at 230.89, 280.61, 401.12, 412.10 and 532.58 eV corresponding to the Mo-3d, C-1s, Mo-3p, N-1s and O-1s, respectively, but some shifting in peaks have been found, which may be due to incomplete and intermediate states at the annealing temperature of 900 °C.<sup>1, 2</sup> Elemental spectrums have been illustrated in detail to evaluate the change and composition of the structure. The molybdenum elemental spectrum of the Mo<sub>2</sub>C-900 showed the binding energies peaks at 228.27, 229.00, 232.38 and 235.46 eV and predicted the existence of molybdenum in different states (Figure S1e). There is no significant difference in some peaks, which corresponds to the similar molybdenum states. The peaks at 228.27 and 229.0

eV corresponded to the  $\text{Mo}^{+2}\text{-}3\text{d}_{5/2}$  and  $\text{Mo}^{+2}\text{-}3\text{d}_{3/2}$  states. The peaks at 232.13 eV revealed to the  $\text{Mo}^{+4}\text{-}3\text{d}_{3/2}$  state of molybdenum, while there is no significant difference at 232.38 and 235.46 eV predicted to the  $\text{Mo}^{+4}\text{-}3\text{d}_{3/2}$  of molybdenum. The surface of the  $\text{Mo}_2\text{C-900}$  was exposed to environmental oxygen but the higher temperature sputtered and reduced the environmental oxygen and precursors as compared to  $\text{Mo}_2\text{C-600}$ .<sup>1-3</sup> The carbon elemental spectrum of the  $\text{Mo}_2\text{C-900}$  showed the binding energies peaks at 284.80, 285.60 and 287.75 eV (Figure S1f). There is a little difference between the first two peaks at 284.80 and 285.60 eV, which is revealed to the C-1s. The peaks at 287.75 eV showed that the surface of the  $\text{Mo}_2\text{C-900}$  was exposed to the environmental surface.<sup>2</sup> Molybdenum and carbon composition was found as 0.13 and 53.16 % in the  $\text{Mo}_2\text{C-600}$ . Molybdenum and carbon composition was 10.99 and 60.98 % in the  $\text{Mo}_2\text{C-900}$ . The composition of the molybdenum was found to be greater in  $\text{Mo}_2\text{C-1200}$  than in  $\text{Mo}_2\text{C-600}$  and  $\text{Mo}_2\text{C-900}$ , which reveals the higher temperature sputter the environmental oxygen and precursors and led to a good structure.

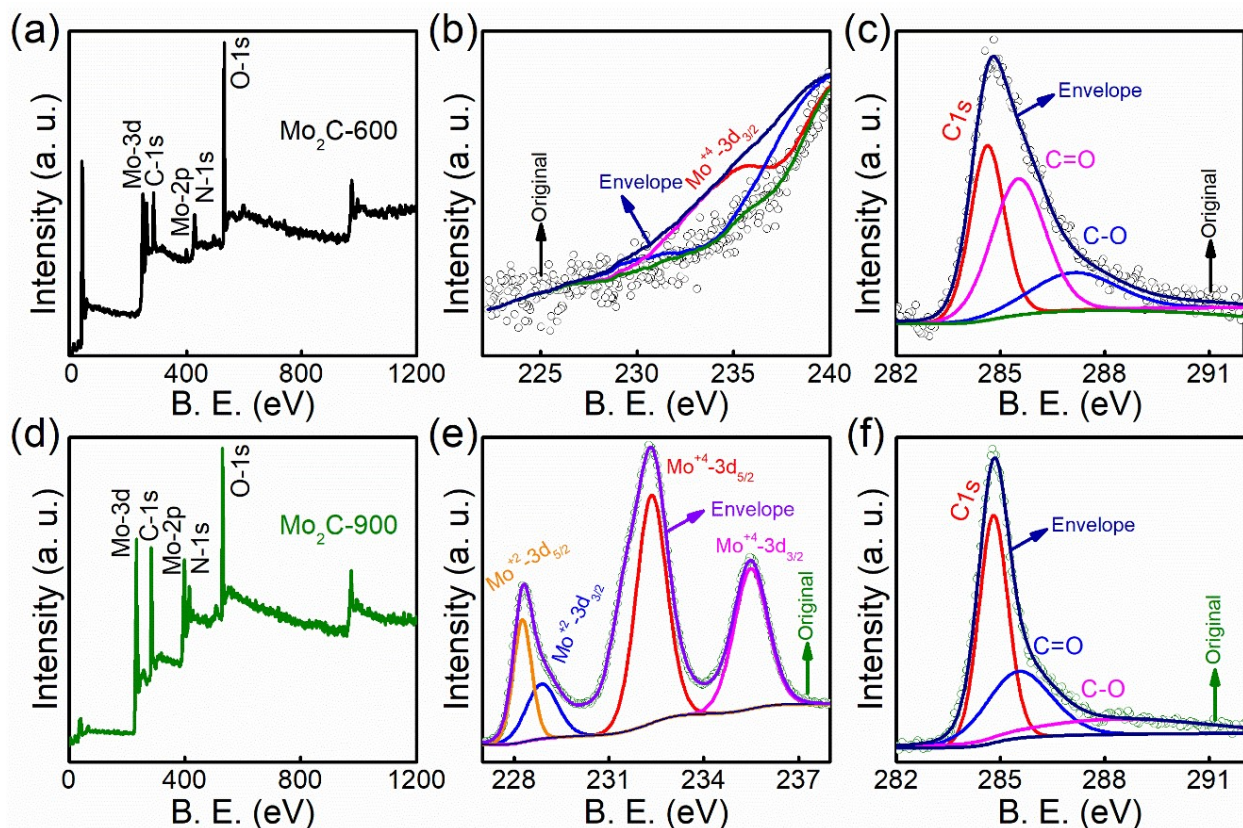


**Figure S1:** XPS spectrum (a) Survey spectrum (b) Molybdenum spectrum and (c) Carbon spectrum for Mo<sub>2</sub>C-600. (d) Survey spectrum (e) Molybdenum spectrum and (f) Carbon spectrum for Mo<sub>2</sub>C-900 nanosheets.

## 2. Morphological analysis

Morphology can significantly boost the electrocatalytic behavior of the electrode structures. Shape and morphological analysis was studied using the SEM and TEM. SEM images reveal that Mo<sub>2</sub>C-600 was irregular. Mo<sub>2</sub>C-600 exhibited a hybrid and different shape, consisting of spherical balls and nanorods. TEM images reveal that Mo<sub>2</sub>C-600 showed the stack and irregular pattern of nanosheets (Figure S2a, b). TEM analysis at higher magnifications reveals that the ratio of the nanosheets was greater for Mo<sub>2</sub>C-600. EDX mapping of the Mo<sub>2</sub>C-600 showed the uniform

distribution of different elements available in the precursors as carbon, nitrogen, oxygen and molybdenum (Figure S2c-f). EDX mapping is also well consistent with the SEM and suggests the distribution of the distribution of different elements in different shapes. Precursors did not react at 600 °C or the employed duration was insufficient to stimulate the reaction. So, the synthesis of Mo<sub>2</sub>C-600 is not successful and it is well manifested with the XRD predictions.

TEM images reveal that Mo<sub>2</sub>C-900 showed well-defined nanosheets (Figure S3a, b), which are well consistent with SEM images. TEM analysis at higher magnifications reveals that the ratio of the nanosheets was greater for Mo<sub>2</sub>C-600. EDX mapping of the Mo<sub>2</sub>C-900 showed the uniform distribution of molybdenum, carbon and oxygen elements (Figure S3c-e). EDX mapping is also well consistent with the SEM and suggests the distribution of the distribution of different elements in the nanosheets like shape and corresponds to Mo<sub>2</sub>C-900 nanosheets.

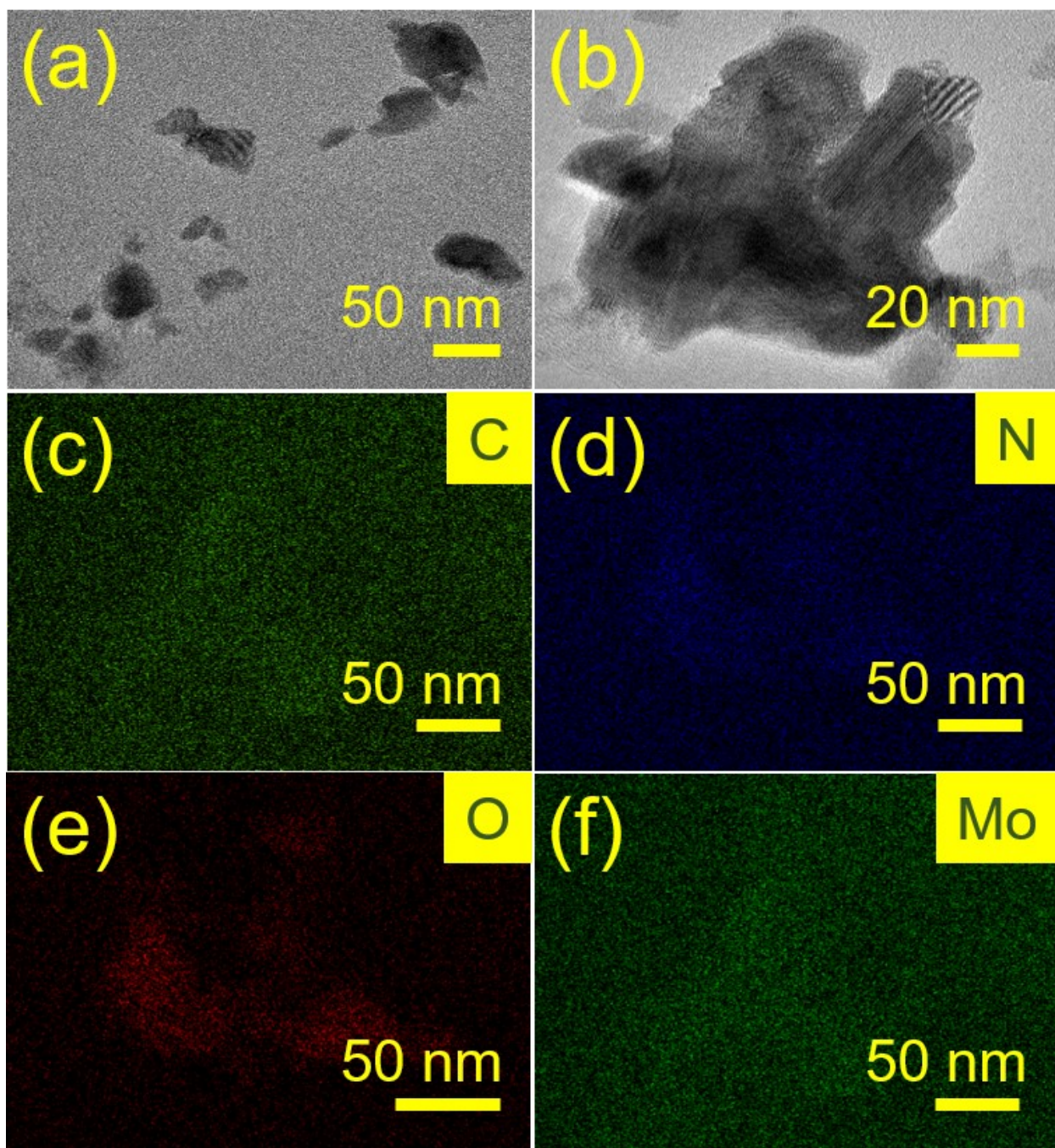


**Figure S2.** TEM images (a, b)  $\text{Mo}_2\text{C}$ -600 hybrid shape. EDX mapping for elemental distribution of (c) carbon element (d) nitrogen element (e) oxygen element and (f) carbon element in  $\text{Mo}_2\text{C}$ -600.

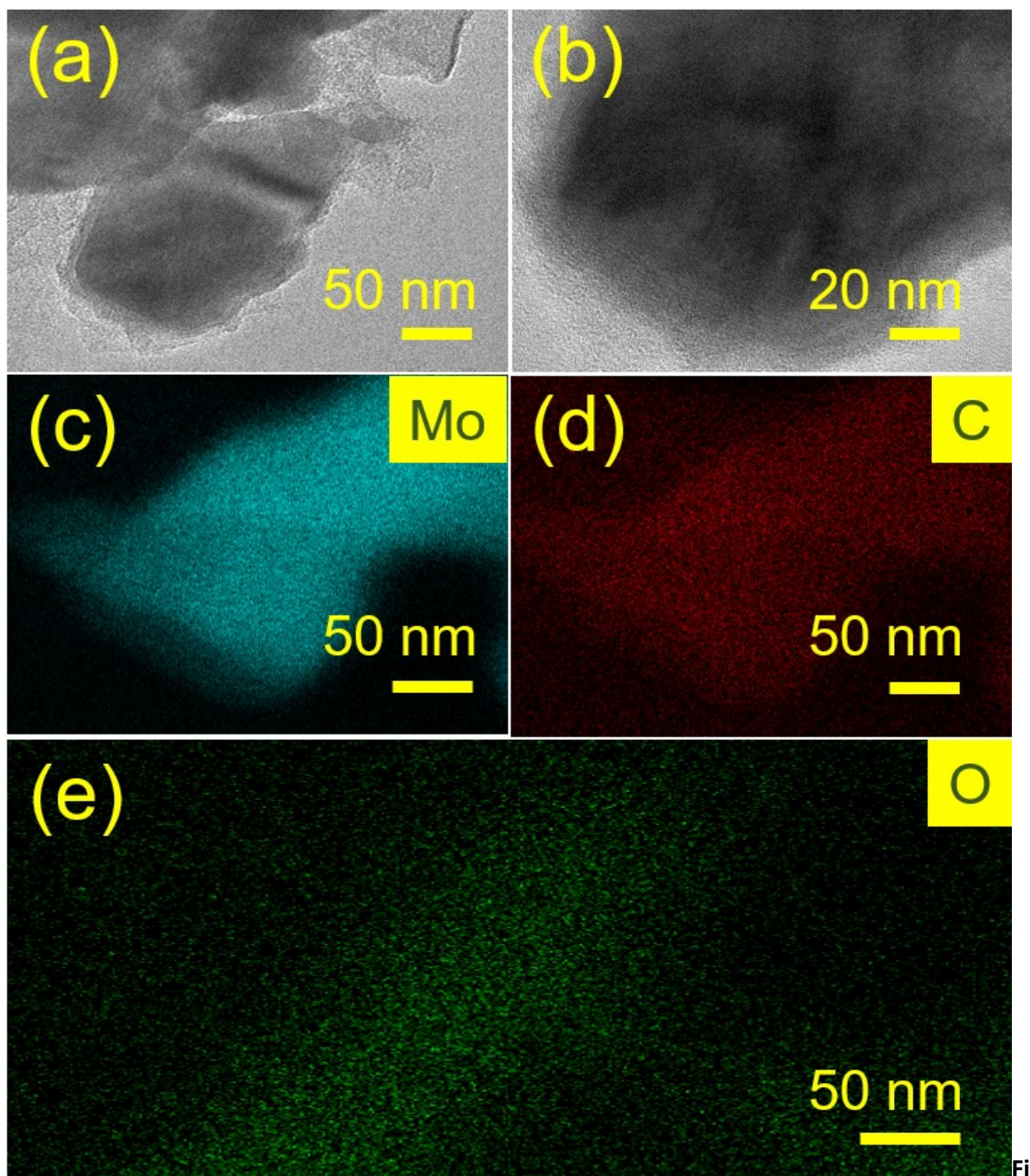


**Figure S3.** TEM images (a, b) Mo<sub>2</sub>C-900 nanosheets. EDX mapping for elemental distribution of (c) molybdenum element (d) carbon element and (e) oxygen element in Mo<sub>2</sub>C-900 nanosheets.

### 3. Electrochemical measurements

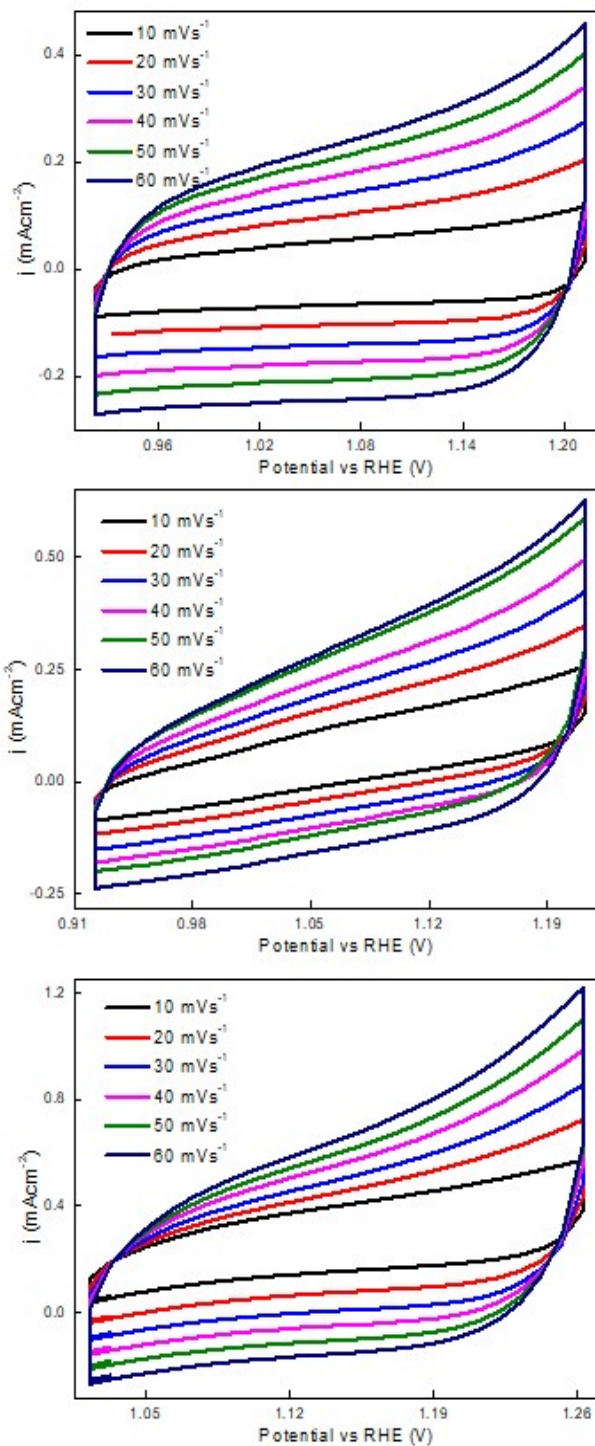


**Figure S4.** CV curves at different scan rates (a) Mo<sub>2</sub>C-600 (b) Mo<sub>2</sub>C-900 nanosheets and (c) carbon element in Mo<sub>2</sub>C-1200 nanosheets in 1 M KOH.

**Table S1.** Summary of specific surface area and electrical conductivity.

S. no.	Electrocatalysts	Specific surface area (m <sup>2</sup> g <sup>-1</sup> )	Electrical conductivity (μΩ cm <sup>-1</sup> )
1	Mo <sub>2</sub> C-600	56.76	2.18
2	Mo <sub>2</sub> C-900	64.47	86.30
3	Mo <sub>2</sub> C-1200	77.46	104.50

**Table S2.** Summary of HER measurements.

S. no.	Electrocatalysts	Electrolytes	η (mV)	Tafel slope (mV dec <sup>-1</sup> )	TOF (s <sup>-1</sup> )
1	Mo <sub>2</sub> C-600	0.5 M H <sub>2</sub> SO <sub>4</sub>	746	137	5.87
		1 M KOH	178	161	169.66
2	Mo <sub>2</sub> C-900 nanosheets	0.5 M H <sub>2</sub> SO <sub>4</sub>	189	115	217.21
		1 M KOH	161	69	197.84
3	Mo <sub>2</sub> C-1200 nanosheets	0.5 M H <sub>2</sub> SO <sub>4</sub>	166	88	304.10
		1 M KOH	139	44	210.75

**Table S3.** Comparative Overpotential and Tafel slopes of Similar electrocatalysts.

S. no.	Electrocatalysts	Strategy	Electrolyte	Overpotential mV	Tafel slope (mV dec <sup>-1</sup> )	Ref.
1	Mo <sub>2</sub> C porous channels	Phosphomolybdic at 950 °C for 2 hours	1 M KOH	110	73.90	<sup>2</sup>
2	Mo <sub>2</sub> C	Two-step processes consisting of hydrothermal and annealing processes	1 M KOH	95		<sup>3</sup>
3	WC		0.1 M KOH	498	105.40	
	WC@NC	Nitrogen doped carbon layer	0.1 M KOH	282	77.30	<sup>4</sup>
4	WC <sub>1-x</sub>	Comparative study	1 KOH	216	122.2	
			0.5 M H <sub>2</sub> SO <sub>4</sub>	247		<sup>5</sup>
5	Mo <sub>0.84</sub> Ni <sub>0.16</sub> -Mo <sub>2</sub> C/NCNFs	Bimetallic alloy-metal carbide heterostructures	1 M KOH	183	71	<sup>6</sup>
6	np-η-MoC nanosheets	Phase transformation	0.5 M H <sub>2</sub> SO <sub>4</sub>	119	53	
			1 M KOH	122	39	<sup>7</sup>
7	α-Mo <sub>2</sub> C-5	Annealing at 590 °C	1 M HClO <sub>4</sub>	126	67	<sup>8</sup>
			1 M KOH	122	41	
8	Mo <sub>2</sub> C-1200 nanosheets	Annealing temperature and electrolytes	0.5 M H <sub>2</sub> SO <sub>4</sub>	166	88	This work
			1 M KOH	139	44	

**Table S4.** Summary of electrochemical surface area ( $A_{\text{ECSA}}$ ).

Scan rate ( $\text{V s}^{-1}$ )	Sqr. of Scan rate ( $\text{V s}^{-1}$ )	$\text{Mo}_2\text{C-600}$	$\text{Mo}_2\text{C-900}$	$\text{Mo}_2\text{C-1200}$
0.01	0.1	114.22	116.96	224.50
0.02	0.141421	96.34	93.78	175.01
0.03	0.173205	87.44	83.40	152.98
0.04	0.20	81.20	77.41	140.30
0.05	0.223607	76.76	73.47	130.11
0.06	0.244949	73.25	69.40	123.67

## References

1. Y. Xu, R. Wang, J. Wang, J. Li, T. Jiao and Z. Liu, *Chemical Engineering Journal*, 2021, **417**, 129233.
2. X. Yang, J. Cheng, X. Yang, Y. Xu, W. Sun and J. Zhou, *Chemical Engineering Journal*, 2023, **451**, 138977.
3. Y. Zheng, Y. Chen, X. Yue and S. Huang, *ACS Sustainable Chemistry & Engineering*, 2020, **8**, 10284-10291.
4. Y. Wang, T. Wang, S. Zhang, X. Meng, Y.-S. He, W. Zhang, Y. Huang and N. Yang, *International Journal of Hydrogen Energy*, 2022, **47**, 314-319.
5. R. Tong, Y. Qu, Q. Zhu, X. Wang, Y. Lu, S. Wang and H. Pan, *ACS Applied Energy Materials*, 2020, **3**, 1082-1088.

6. L. Ying, S. Sun, W. Liu, H. Zhu, Z. Zhu, A. Liu, L. Yang, S. Lu, F. Duan, C. Yang and M. Du, *Renewable Energy*, 2020, **161**, 1036-1045.
7. C. Tang, H. Zhang, K. Xu, Q. Zhang, J. Liu, C. He, L. Fan and T. Asefa, *Journal of Materials Chemistry A*, 2019, **7**, 18030-18038.
8. J. Shi, L. Hu, J. Liu, M. Chen, C. C. Li, G. Guan, Y. Ma and T. Wang, *Journal of Materials Chemistry A*, 2022, **10**, 11414-11425.